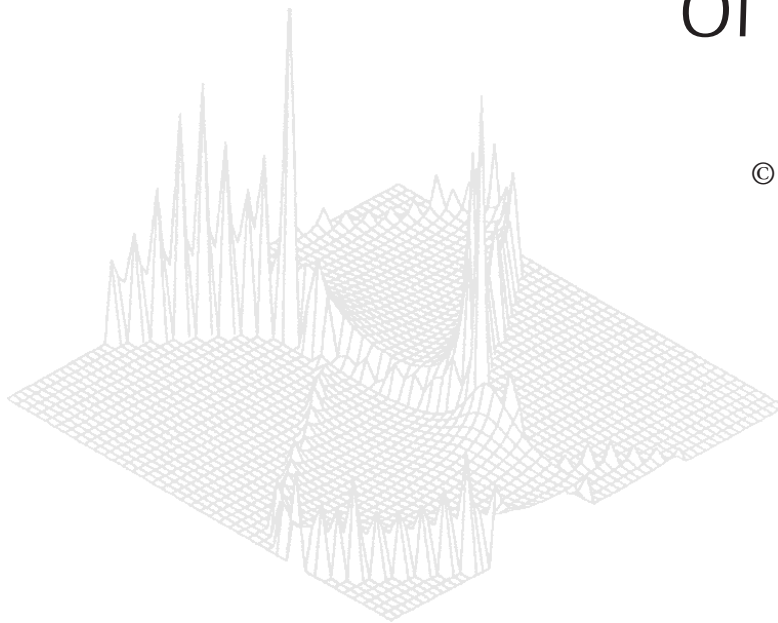

C S I R O P U B L I S H I N G

Australian Journal of Physics

Volume 50, 1997
© CSIRO Australia 1997



A journal for the publication of
original research in all branches of physics

www.publish.csiro.au/journals/ajp

All enquiries and manuscripts should be directed to

Australian Journal of Physics

CSIRO PUBLISHING

PO Box 1139 (150 Oxford St)

Collingwood

Vic. 3066

Australia

Telephone: 61 3 9662 7626

Facsimile: 61 3 9662 7611

Email: peter.robertson@publish.csiro.au



Published by **CSIRO PUBLISHING**
for CSIRO Australia and
the Australian Academy of Science



Quasiparticle Lifetimes and the Conductivity Scattering Rate*

F. Marsiglio^{A,B,C,D} and *J. P. Carbotte*^{B,C}

^A Neutron & Condensed Matter Science, AECL, Chalk River Laboratories, Chalk River, Ontario K0J 1J0, Canada.

^B Department of Physics & Astronomy, McMaster University, Hamilton, Ontario L8S 4M1, Canada.

^C Canadian Institute for Advanced Research, McMaster University, Hamilton, Ontario L8S 4M1, Canada.

^D Present address: Department of Physics, University of Alberta, Edmonton, Alberta T6G 2J1, Canada.

Abstract

We compute the single-particle inverse lifetime, along with the conductivity-derived scattering rate, for a metallic system in an s-wave superconducting state. When both electron–phonon and electron–impurity scattering are included, we find that while these scattering rates are in qualitative agreement, in general quantitative agreement is lacking. We also derive results for the quasiparticle lifetime within the BCS framework with impurity scattering, which makes it clear that impurity scattering is suppressed for electrons near the Fermi surface in the superconducting state.

1. Introduction

The quasiparticle lifetime is a concept which is useful for clarifying the nature of the system of interest, i.e. is it a Fermi versus marginal Fermi versus a Luttinger liquid?, etc. (Bedell *et al.* 1990). Various techniques are available for measuring lifetimes (Kaplan *et al.* 1976); perhaps the most direct is through tunnel junction detection (Narayanamuti *et al.* 1978). In this paper we analyse electron scattering rates, as measured by microwave and far-infrared conductivity measurements, and examine their relationship to quasiparticle lifetimes. We will reserve the name ‘quasiparticle lifetime’ to refer to the single-particle property to be defined technically in the next section. In contrast we will use the term ‘scattering rate’ or ‘scattering lifetime’ to refer to a property derived from a response function, such as the optical conductivity in this case. The experimental results for $\text{YBaCu}_3\text{O}_{7-x}$ (Bonn *et al.* 1992, 1993) and their theoretical implications (Bonn *et al.* 1993, 1994; Berlinsky *et al.* 1993; Klein 1994) have been discussed extensively in the literature. In these works the microwave conductivity was used to extract information about quasiparticle scattering; it is commonly and often tacitly presumed that the ‘lifetime’ (inverse scattering rate) derived from these sorts of measurements is closely related to the quasiparticle lifetime, as derived from the single-particle

* Refereed paper based on a contribution to the Fifth Gordon Godfrey Workshop on Superconductivity held at the University of New South Wales, Sydney, in November 1995.

Green function. In this work we explore this relationship and compute both the single-particle lifetime and the two-particle scattering rate, including both electron-impurity scattering and electron-phonon scattering. The latter involves inelastic scattering processes and introduces significant complications. We use an Eliashberg formalism to analyse this problem, with some further approximations which will be made clear in the relevant sections. A similar approach has already been used to analyse the normal state problem (Shulga *et al.* 1991; Marsiglio and Carbotte 1995). Here, certain aspects of quasiparticle lifetimes are clarified and the analysis is extended to the superconducting state, following our recent work on optical conductivity (Marsiglio and Carbotte 1995; Marsiglio *et al.* 1996).

We will proceed by carefully defining the single-particle lifetime. We review two ways in which conductivity data can be used to extract a scattering rate, one based on the two-fluid model, and the other based on a straightforward Drude fit to the low frequency conductivity. The instances in which these procedures yield a qualitative or quantitative facsimile of the quasiparticle inverse lifetime will be clarified. In this way, one can evaluate the usefulness of the two-fluid hypothesis, for example, in systems with both elastic and inelastic scattering channels.

This paper is divided into two sections. The first reviews quasiparticle lifetimes, which are calculated from the single-particle Green function. In the normal state the single-particle equations for electron-impurity scattering (in the Born approximation) and electron-phonon scattering are well known (Mahan 1981, 1987; Allen and Mitrović 1982; Grimvall 1981). In the superconducting state, we first examine the BCS case with electron-impurity scattering. By ‘BCS’ we mean the limit where the pairing interaction is instantaneous, and in this case local, i.e. the gap function is independent of frequency and momentum. The single-particle spectral function is given analytically, showing explicitly the role of the so-called BCS coherence factors which are somewhat disguised in the clean limit. When impurity scattering is included, such an expression should be used in lieu of the more commonly adopted phenomenological form found in standard texts (Schrieffer 1983). When inelastic electron-phonon scattering is included in the problem, perturbative methods within the Eliashberg framework are used. This follows closely the work in Kaplan *et al.* (1976); however, here we discuss the quasiparticle lifetimes in the presence of *both* impurity and phonon scattering.

The second section elucidates two methods recently used to extract scattering rates from optical and microwave conductivity measurements, and how these relate to the quasiparticle inverse lifetime. We should make it clear at the start that the calculation we use for the optical conductivity omits vertex corrections. The main result of this is that the ‘ $1 - \cos\theta$ ’ factor that occurs in a Boltzmann formulation of transport properties is absent (Mahan 1981, 1987), so in fact, when theoretical comparisons between the quasiparticle lifetime and the conductivity-derived scattering rate are made, the agreement will in general be better than it would be, given an exact calculation. Conversely, poor agreement between these two quantities in the theory would almost certainly result in poor agreement between the two measured quantities.

2. Quasiparticle Lifetimes

Quasiparticle lifetimes in clean electron-phonon superconductors were discussed long ago by Kaplan *et al.* (1976). Before proceeding to their relationship with

the optical conductivity we give a brief review of the formalism (Kaplan *et al.* 1976; Nicol 1991). In the normal state the quasiparticle has energy and lifetime defined by the pole of the single-particle retarded Green function, i.e. the zero of

$$G^{-1}(k, \omega + i\delta) = \omega - \epsilon_k - \Sigma(\omega + i\delta), \quad (1)$$

where $\Sigma(\omega + i\delta)$ is the electron self-energy. More specifically the solution ω_k , where $\omega_k = \epsilon_k + \Sigma(\omega_k + i\delta)$, defines the quasiparticle energy E_k and inverse lifetime Γ_k by

$$\omega_k \equiv E_k - i\Gamma_k/2. \quad (2)$$

Similarly, in the superconducting state, the inverse quasiparticle lifetime is defined by (twice) the imaginary part of the pole in the single-particle Green function. The diagonal component of the single-particle Green function is (Scalapino 1969)

$$G_{11}(k, \omega) = \frac{\omega Z(\omega) + \epsilon_k}{\omega^2 Z^2(\omega) - \epsilon_k^2 - \phi^2(\omega)}, \quad (3)$$

where $Z(\omega)$ and $\phi(\omega)$ are the renormalisation and pairing functions given by solutions to the Eliashberg equations (Eliashberg 1960; Scalapino 1969; Marsiglio *et al.* 1988) which are repeated here for convenience:

$$\begin{aligned} \phi(\omega) = \pi T \sum_{m=-\infty}^{\infty} & [\lambda(\omega - i\omega_m) - \mu^*(\omega_c)\theta(\omega_c - |\omega_m|)] \frac{\phi_m}{\sqrt{\omega_m^2 Z^2(i\omega_m) + \phi_m^2}} \\ & + i\pi \int_0^{\infty} d\nu \alpha^2 F(\nu) \left\{ [N(\nu) + f(\nu - \omega)] \frac{\phi(\omega - \nu)}{\sqrt{\tilde{\omega}^2(\omega - \nu) - \phi^2(\omega - \nu)}} \right. \\ & \left. + [N(\nu) + f(\nu + \omega)] \frac{\phi(\omega + \nu)}{\sqrt{\tilde{\omega}^2(\omega + \nu) - \phi^2(\omega + \nu)}} \right\} \end{aligned} \quad (4)$$

and

$$\begin{aligned} \tilde{\omega}(\omega) = \omega + i\pi T \sum_{m=-\infty}^{\infty} & \lambda(\omega - i\omega_m) \frac{\omega_m Z(i\omega_m)}{\sqrt{\omega_m^2 Z^2(i\omega_m) + \phi_m^2}} \\ & + i\pi \int_0^{\infty} d\nu \alpha^2 F(\nu) \left\{ [N(\nu) + f(\nu - \omega)] \frac{\tilde{\omega}(\omega - \nu)}{\sqrt{\tilde{\omega}^2(\omega - \nu) - \phi^2(\omega - \nu)}} \right. \\ & \left. + [N(\nu) + f(\nu + \omega)] \frac{\tilde{\omega}(\omega + \nu)}{\sqrt{\tilde{\omega}^2(\omega + \nu) - \phi^2(\omega + \nu)}} \right\}, \end{aligned} \quad (5)$$

where $\tilde{\omega}(\omega) \equiv \omega Z(\omega)$. Here $N(\nu)$ and $f(\nu)$ are the Bose and Fermi distribution functions, respectively. The electron-phonon spectral function is given by $\alpha^2 F(\nu)$, and its Hilbert transform is $\lambda(z)$. The Coulomb repulsion parameter is $\mu^*(\omega_c)$ with cutoff ω_c . A negative value for this parameter can be used to model some BCS attraction of unspecified origin. The renormalisation and pairing functions are first obtained on the imaginary axis at the Matsubara frequencies,

i.e. $\omega = i\omega_n \equiv i\pi T(2n - 1)$, with $\phi_m \equiv \phi(i\omega_m)$, by setting the complex variable ω in these equations to the Matsubara frequencies (Owen and Scalapino 1971; Rainer and Bergmann 1974). Then the equations are iterated as written, with ω set to a frequency on the real axis. Note that the square roots with complex arguments are defined to have a positive imaginary part.

Actually, these functions are obtained at frequencies just above the real axis, and then, in principle, the pole is given by the zero of the denominator continued to the lower half-plane. However, since the solutions are readily known only along certain lines in the complex plane (e.g. the imaginary axis or just above the real axis) we follow previous authors and look for the pole perturbatively. That is, we write $\omega \equiv E - i\Gamma$, and linearise the imaginary part so that (Scalapino 1969; Kaplan *et al.* 1976)

$$\Gamma(E) = \frac{EZ_2(E)}{Z_1(E)} - \frac{\phi_1(E)\phi_2(E)}{EZ_1^2(E)}. \quad (6)$$

Note that E is determined by equating the real parts (again linearising in imaginary components), which yields

$$E = \sqrt{\frac{\epsilon_k^2 + \phi_1^2(E)}{Z_1^2(E)}}. \quad (7)$$

In the normal state, $\phi(\omega) \equiv 0$, and equation (5) simplifies to the known normal state result (Allen and Mitrović 1982; Grimvall 1981). The quasiparticle energy and lifetime are given by equations (7) and (6), which yield in the low energy limit (Allen and Mitrović 1982; Grimvall 1981):

$$E \approx \frac{\epsilon_k}{1 + \lambda^*(T)}, \quad (8)$$

$$\Gamma(E = 0) \approx \frac{\frac{1}{\tau} + 4\pi \int_0^\infty d\nu \alpha^2 F(\nu) [N(\nu) + f(\nu)]}{1 + \lambda^*(T)}, \quad (9)$$

where $f(\nu)$ is the Fermi function and

$$\lambda^*(T) \approx -\frac{1}{\pi T} \int_0^\infty d\nu \alpha^2 F(\nu) \text{Im} \psi' \left(\frac{1}{2} + i \frac{\nu}{2\pi T} \right). \quad (10)$$

Typical results for various electron-phonon spectral functions are shown in Fig. 1 for the clean limit over a wide range of temperatures.

Returning to the superconducting state, at the Fermi surface $\epsilon_k \equiv 0$ so (7) gives $E = \phi_1(E)/Z_1(E) \equiv \Delta_1(E)$, which becomes the definition for the lowest energy excitation, i.e. the gap in the excitation spectrum. It has become common practice to consider E as an independent variable, and then to study $\Gamma(E)$ as a function of E . In Fig. 2 we show $\Gamma(E)$ versus E for various temperatures, using a Debye model spectrum. It is clear that the scattering rate near the gap

edge (shown by the arrow) decreases very quickly as the temperature decreases. Note that $\Gamma(E)$ actually becomes negative at intermediate temperatures near $E \approx 10$ meV. This is real (i.e. not a numerical artifact) and is simply a property of the function $\Gamma(E)$ given by (6) through the linearisation procedure. The true pole in (3) will always have a negative imaginary part (i.e. Γ is positive).

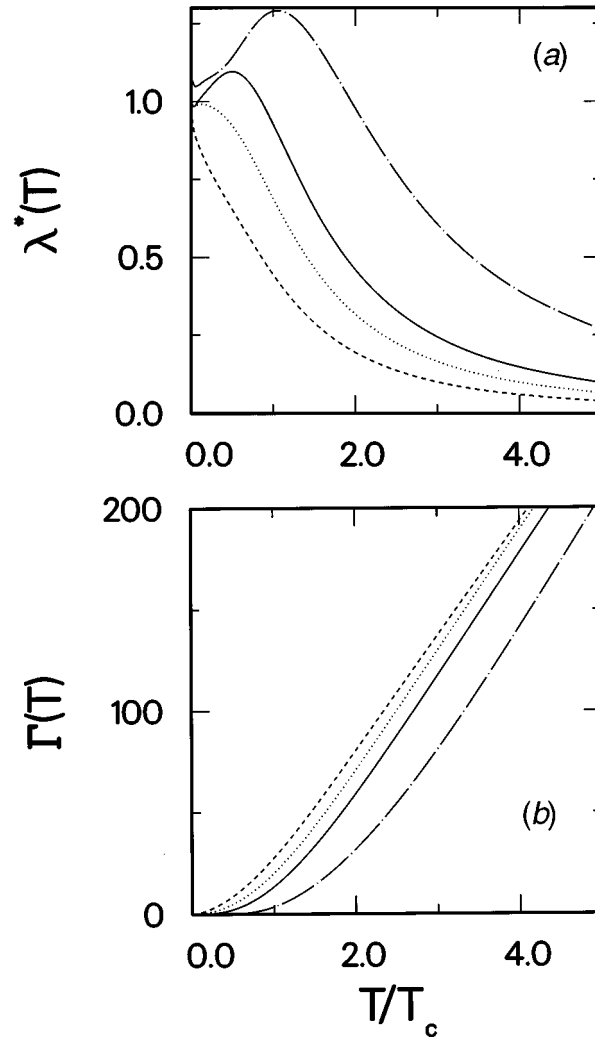


Fig. 1. (a) Mass enhancement parameter, as defined by equation (10) in the text, versus reduced temperature T/T_c , for various electron-phonon spectral functions. In all cases $T_c = 100$ K. The four spectra used are a Debye spectrum (solid line), linear spectrum (dotted line), a spectrum proportional to $\sqrt{\nu}$ (dashed line), and a triangular spectrum (dot-dashed line). In all cases the strength is such that $\lambda = 1$. In the first three cases a cutoff frequency equal to 30 meV was used. In the last case, the spectrum starts at 34.8 meV and is cut off at 35.5 meV. (b) Inverse lifetime $\Gamma(T)$ (in meV) versus reduced temperature for the same spectra as in (a). Note the different low temperature behaviour, depending on the low frequency characteristics of the electron-phonon spectrum used.

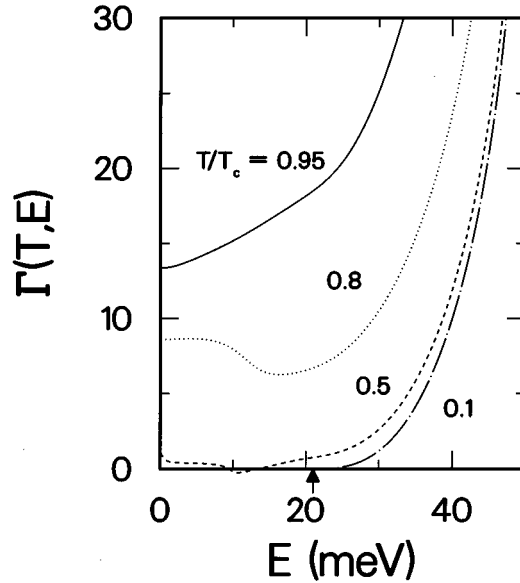


Fig. 2. Scattering rate $\Gamma(T, E)$ (in meV) versus E (in meV) for various temperatures in the superconducting state. The zero temperature gap at the Fermi surface is indicated by the arrow. Note that for $T/T_c = 0.5$ the function plotted actually becomes negative (near 10 meV). The physical pole occurs at an energy E , where $\Gamma(T, E)$ is always positive, however.

What happens when both the BCS limit and the clean limit are taken? Then $Z_2(E) \rightarrow 0$ and $\phi_2(E) \rightarrow 0$, i.e. the functions involved in the solution are pure real, with $Z_1(E) \rightarrow 1$ and $\phi_1(E) \rightarrow \Delta(T)$, where $\Delta(T)$ is obtained self-consistently from the BCS equation. Clearly then the quasiparticle energy is $E = \sqrt{\epsilon_k^2 + \Delta^2}$ and the scattering rate, $\Gamma = 0$. Thus, within the BCS approximation in the clean limit the quasiparticle states are infinitely long-lived, as there is no means by which a quasiparticle can decay. With either impurity or phonon scattering, quasiparticle decay becomes possible. In this way the BCS approximation in the clean limit is pathological.

Let us first examine the situation where only electron-impurity scattering is present, i.e. no phonon scattering occurs. Then the pairing and renormalisation function become

$$\begin{aligned}\phi(\omega) &= \phi_{cl}(\omega) + \frac{i}{2\tau} \frac{\phi(\omega)}{\sqrt{\omega^2 Z^2(\omega) - \phi^2(\omega)}}, \\ Z(\omega) &= Z_{cl}(\omega) + \frac{i}{2\tau} \frac{Z(\omega)}{\sqrt{\omega^2 Z^2(\omega) - \phi^2(\omega)}},\end{aligned}\quad (11)$$

where the subscript 'cl' refers to the clean limit and $1/\tau$ is the (normal) impurity scattering rate. The gap function is defined

$$\Delta(\omega) = \phi(\omega)/Z(\omega) \quad (12)$$

and is independent of impurity scattering. In the BCS limit, we have

$$\phi(\omega) = \Delta + \frac{i}{2\tau} \frac{\Delta \operatorname{sgn}\omega}{\sqrt{\omega^2 - \Delta^2}}, \quad Z(\omega) = 1 + \frac{i}{2\tau} \frac{\operatorname{sgn}\omega}{\sqrt{\omega^2 - \Delta^2}}. \quad (13)$$

As before, using the perturbative approach, the quasiparticle energy is given by $E = \sqrt{\epsilon_k^2 + \Delta^2}$, but the scattering rate is now (Pethick and Pines 1986)

$$\Gamma = \frac{1}{\tau} \frac{\sqrt{E^2 - \Delta^2}}{|E|} = \frac{1}{\tau} \frac{|\epsilon_k|}{\sqrt{\epsilon_k^2 + \Delta^2}}. \quad (14)$$

Equation (14) shows that at the Fermi surface impurities are ineffectual for electron scattering, i.e. this is another manifestation of Anderson's (1959) theorem. This happens abruptly at T_c ; as soon as a gap develops the scattering rate becomes zero. Away from the Fermi surface the scattering rate is reduced from its value in the normal state. In particular, well away from the Fermi surface the scattering rate in the superconducting state approaches the normal state rate. This behaviour is illustrated in Fig. 3.

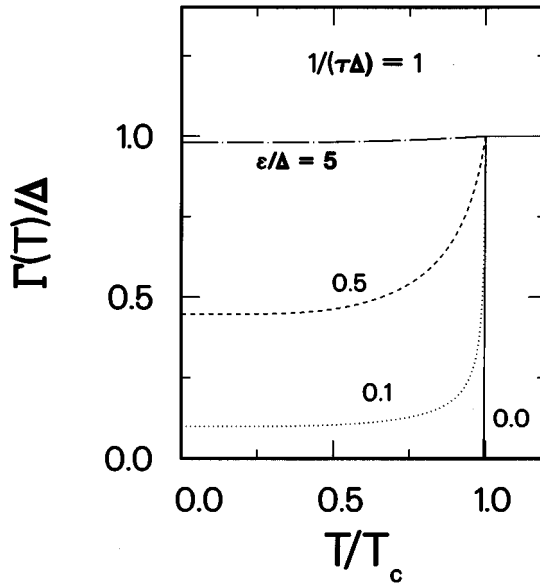


Fig. 3. Scattering rate normalised to the zero temperature gap $\Gamma(T, E)/\Delta$ versus reduced temperature T/T_c , for various quasiparticle energies ϵ . These are computed using the perturbative expansion (14). The impurity scattering rate is $1/(\tau\Delta) = 1$. Note that on the Fermi surface (solid curve), the scattering rate is zero immediately below T_c .

The calculations in Fig. 3 rely on a perturbative search for the pole in the lower half-plane, as given by (6). A more rigorous calculation reveals poles 'within the gap', but these do not appear in the spectral function because of coherence factors. This can be seen by rewriting (6) as

$$G_{11}(k, \omega) = \frac{1}{2} \left(1 + \frac{\omega}{\sqrt{\omega^2 - \Delta^2}} \right) \frac{1}{\sqrt{\omega^2 - \Delta^2} - \epsilon_k + \frac{i}{2\tau} \operatorname{sgn}\omega} - \frac{1}{2} \left(1 - \frac{\omega}{\sqrt{\omega^2 - \Delta^2}} \right) \frac{1}{\sqrt{\omega^2 - \Delta^2} + \epsilon_k + \frac{i}{2\tau} \operatorname{sgn}\omega}. \quad (15)$$

The coherence factors, $(1 \pm \frac{\omega}{\sqrt{\omega^2 - \Delta^2}})$, are such that the spectral function, $A(k, \omega) \equiv -\frac{1}{\pi} \operatorname{Im} G(k, \omega)$, is zero for $|\omega| < \Delta$, independent of the impurity scattering rate, as can be readily verified explicitly from (15). On the other hand the precise pole of the Green function is given by solving for $\omega = E - i\Gamma/2$ in the two coupled equations

$$E^2 - (\Gamma/2)^2 = \Delta^2 + \epsilon_k^2 - (1/2\tau)^2, \quad (16)$$

$$\Gamma = \frac{|\epsilon_k|}{|E|} \frac{1}{\tau}. \quad (17)$$

For $1/\tau = 0$ the solution is as before, $E = E_k \equiv \sqrt{\epsilon_k^2 + \Delta^2}$, and $\Gamma = 0$. For finite impurity scattering, however, the solution depends on $1/(2\tau\Delta)$ at the Fermi surface ($\epsilon_k = 0$):

$$E = \sqrt{\Delta^2 - (1/2\tau)^2}, \quad \Gamma = 0 \quad \text{for} \quad 1/(2\tau\Delta) < 1, \quad (18)$$

$$E = 0, \quad \Gamma = \sqrt{(1/\tau)^2 - (2\Delta)^2} \quad \text{for} \quad 1/(2\tau\Delta) > 1. \quad (19)$$

In either case the solution has a real part that lies within the gap, that is, the quasiparticle residue at the pole is zero. The ‘relevant’ energies (i.e. for which the residue is non-zero) are $|E| > \Delta$, and then the scattering rate given by (17) agrees with the linearised solution (6). However, the quantity $\Gamma(E)$ is only physically meaningful when it is evaluated at the pole energy, which occurs below the gap value, so in the ‘relevant’ region $\Gamma(E)$ is merely a well-defined function. Away from the Fermi surface the quasiparticle energy requires the solution of a quadratic equation and E may lie below or above the gap, depending on ϵ_k and $1/\tau$. Once more solutions with $|E| < \Delta$ have zero spectral weight. In Fig. 4 we show the (a) real and (b) imaginary parts of the pole for some typical parameters. As can be seen, some atypical behaviour can occur as a function of temperature, for example when $\epsilon_k = 0$. As the temperature is lowered the pole moves from a point on the negative imaginary axis to the origin (near $T/T_c = 0.8$) and then moves along the real axis towards $E = \sqrt{\Delta^2 - (1/2\tau)^2}$. Nonetheless, comparison of Fig. 4b with Fig. 3 shows that the perturbative is in qualitative agreement with the non-perturbative solution.

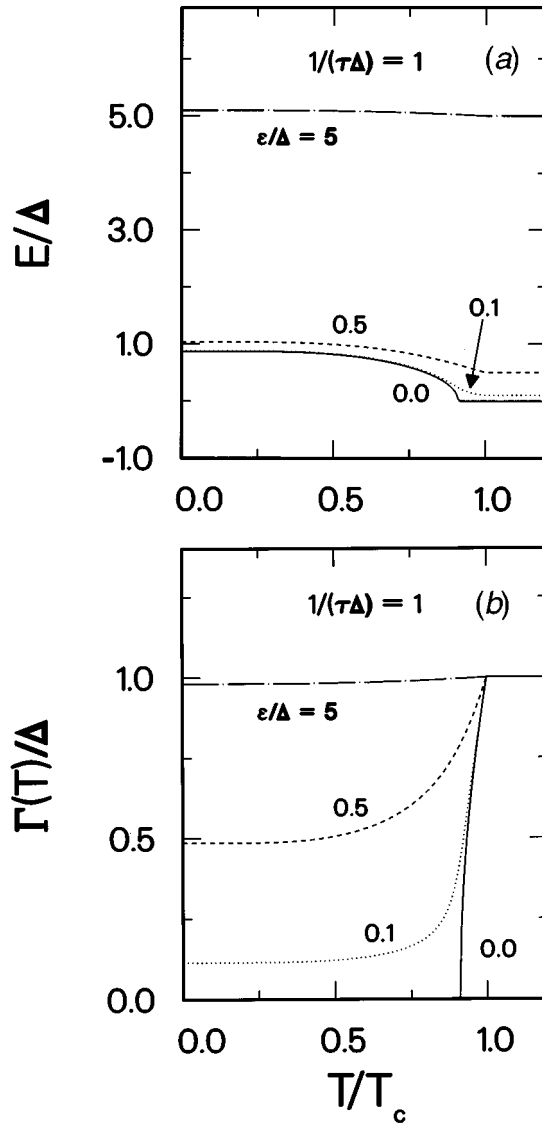


Fig. 4. (a) Real and (b) imaginary parts of the quasiparticle pole versus reduced temperature T/T_c , with $1/(\tau\Delta) = 1$ and various quasiparticle energies. These are computed non-perturbatively from equations (16) and (17). Note that at the Fermi surface the quasiparticle energy has an abrupt onset at a temperature somewhat *below* T_c . The results in (b) are similar to those in Fig. 3, except that at the Fermi surface the decrease in scattering rate below T_c is not as abrupt.

Coherence factors are known to play an important role for two-particle response functions (such as the NMR relaxation rate or the microwave conductivity). In particular they lead to the Hebel–Slichter (1959) singularity in the NMR relaxation rate. However, they have largely been ignored in single-particle functions. Equation (15) shows, however, that the coherence factors play a very important role in the single-particle spectral function, in that they maintain a

gap equal to Δ , even when impurities cause the single-particle pole to have a real part whose value lies in the gap.

The frequency dependence of the spectral function is shown in Fig. 5. For energies close to the Fermi surface the spectral function is dominated by the square root singularity at the gap edge, which comes from the coherence factors rather than the single-particle pole. For larger energies the peak present is due to the pole and differs from the normal state spectral function only at low frequencies.

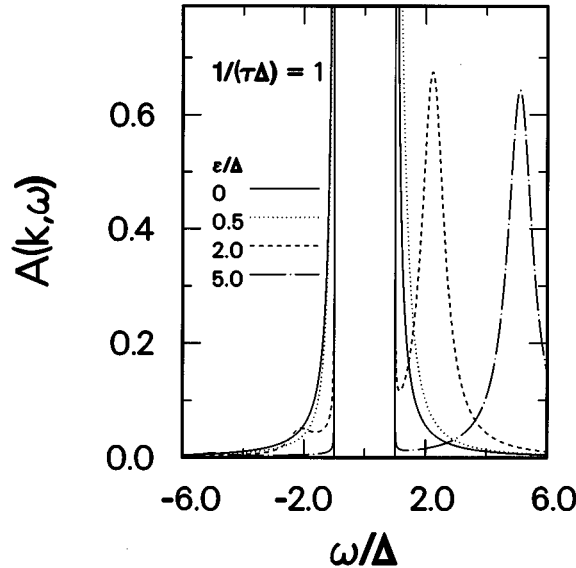


Fig. 5. Single-particle spectral function $A(k, \omega)$ versus normalised frequency ω/Δ , with $1/(\tau\Delta) = 1$, for various quasiparticle energies ϵ/Δ . The Fermi surface result (solid curve) has particle-hole symmetry. The result for $\epsilon/\Delta = 0.5$ would have a peak within the gap (between -1 and 1) except that the coherence factors in (15) give zero residue for the gap region. As the quasiparticle energy increases, the spectral function begins to resemble the normal state spectral function. Small square-root singularities still exist, nonetheless at the particle and hole gap edges.

We return now to the strong coupling case. In the superconducting state, we do not have access to the analytic continuation of the Green function to the lower half-plane. [It is true that we can attempt a representation through Padé approximations, as has often been done in the past, to analytically continue functions from the imaginary axis to the real axis. However, these are notorious for producing spurious poles (Marsiglio *et al.* 1988).] We thus follow Karakozov *et al.* (1975), and use an expansion near $\omega = 0$. We also follow Kaplan *et al.* (1976) and henceforth use (6) for the scattering rate, noting that while the energy E at which $\Gamma(E)$ is evaluated ought, in principle, to be computed self-consistently as was done in BCS, i.e. equations (16) and (17), in practice we will choose the relevant energy, and so treat energy as an independent variable.

Karakozov *et al.* (1975) pointed out that at any finite temperature the solutions to the Eliashberg equations have the following low frequency behaviour:

$$Z(\omega) \approx Z_1 + \frac{i\gamma_2}{\omega}, \quad (20)$$

$$\Delta(\omega) \approx \delta_1\omega^2 - i\delta_2\omega, \quad (21)$$

where Z_1, γ_2, δ_1 and δ_2 are real (positive) constants. This implies that a quasiparticle pole exists with

$$E \approx \frac{\epsilon_k}{Z_1 \sqrt{1 + \delta_2^2}}, \quad (22)$$

$$\Gamma \approx \frac{1}{Z_1} \left(4\pi \int_0^\infty d\nu \alpha^2 F(\nu) g(\nu) [N(\nu) + f(\nu)] + \frac{g(0)}{\tau} \right), \quad (23)$$

where we have used (6) and assumed $E \rightarrow 0$ (i.e. we are near the Fermi surface). In (23) $g(\nu)$ is the single electron density of states in the superconducting state,

$$g(\nu) = \text{Re} \left(\frac{\nu}{\sqrt{\nu^2 - \Delta^2}} \right), \quad (24)$$

which is non-zero for $\nu = 0$ at any finite temperature (Karakozov *et al.* 1975; Marsiglio and Carbotte 1991; Allen and Rainer 1991). In Fig. 6 we show the quasiparticle scattering rate $\Gamma(T, E = 0)$ versus T/T_c for various impurity scattering rates $1/\tau$ in the superconducting state. The normal state result is also shown for reference. Note that in the clean limit there is an enhancement just below T_c in the superconducting state, but at low temperatures there is an exponential suppression, compared to the power law behaviour observed in the normal state. When impurity scattering is present there is an immediate suppression below T_c (a knee is still present, however, in the superconducting state). It is clear that at low temperatures the superconducting state is impervious to impurity scattering, as one would expect.

Is $\Gamma(T, E=0)$ the relevant inverse lifetime by which properties of the superconducting state can be understood? Strictly speaking the answer is no, particularly at low temperatures, where the spectral function essentially develops a gap for low energies. In Fig. 7 we plot the spectral function at the Fermi surface $A(k_F, \omega)$ for various temperatures (Marsiglio and Carbotte 1991). While no true gap exists at any finite temperature, it is clear that for low temperatures the spectral weight at low frequency is exponentially suppressed. Thus we have a situation similar to that in BCS theory, where the quasiparticle pole occurs at an energy where the spectral weight is essentially zero. It is more relevant to inquire about the scattering rate (as defined by equation 6) evaluated above the 'gap-edge' where a large spectral weight is present, and quasiparticles are more likely to be populated (as in detector applications). When impurities are added the spectral peak is broadened, even at low temperatures, as shown in Fig. 8 for an intermediate temperature, $T/T_c = 0.5$. However, the lineshape is very asymmetric as a gap remains at low frequencies (particularly prominent at low temperatures).

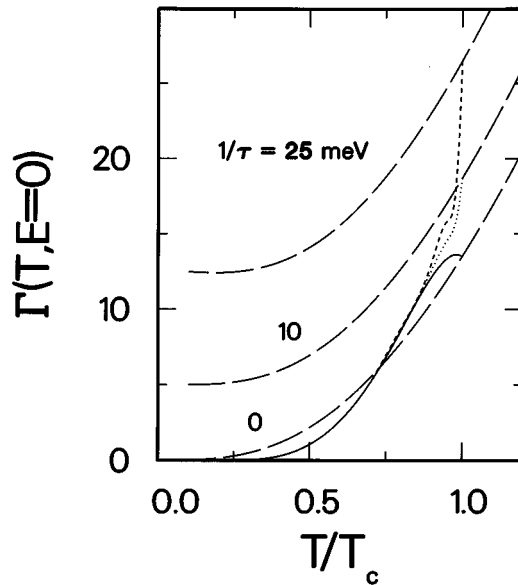


Fig. 6. Quasiparticle scattering rate $\Gamma(T, E=0)$ versus T/T_c for various impurity scattering rates $1/\tau$, in both the superconducting and normal (long-dashed curves) states. In the clean limit (solid curve) there is an enhancement immediately below T_c . When impurity scattering is present, this scattering is immediately suppressed in the superconducting state, as shown by the dotted and dashed curves. Below a temperature of about $0.8T_c$ the scattering rate is independent of the amount of impurity scattering present in the normal state. A Debye electron-phonon spectrum was used with $\lambda = 1$ and cutoff frequency $\omega_D = 30$ meV.

Fig. 7 demonstrates that the relevant energy is a function of temperature. In Fig. 9 we plot $\Gamma(T, E=\Delta(T))$ versus T/T_c , where $\Delta(T)$ is determined from the relation (at the Fermi surface)

$$E = \text{Re}\Delta(E, T). \quad (25)$$

By (25) we understand that the $E = 0$ solution is excluded (similarly the very low energy solution is also excluded). We are interested in the conventional solution which gives rise to the peak in the spectral function illustrated in Fig. 7 or 8. If no non-zero solution is present (as is the case near T_c) then we utilise the $E = 0$ solution. Note that in this case care must be taken when obtaining the $E \rightarrow 0$ limit of (6). Also there is present in this definition a discontinuity at some temperature near T_c , which is where a nonzero solution first appears. In this way we hope to show the scattering rate at an energy where the spectral weight is large, and therefore of most relevance to observables. At any rate, it is clear by comparing Fig. 9 to Fig. 6 (see also Fig. 2) that there is very little difference in the scattering rate in the gap region of energy. However, as the energy increases beyond the gap the scattering rate increases, resulting in short 'lifetimes', even at zero temperature (Kaplan *et al.* 1976). Thus, while we have argued that the quasiparticle lifetime corresponding to the pole of the Green function is of limited use because the quasiparticle residue there is zero, in practice the close correspondence between Fig. 9 and Fig. 6 illustrates that

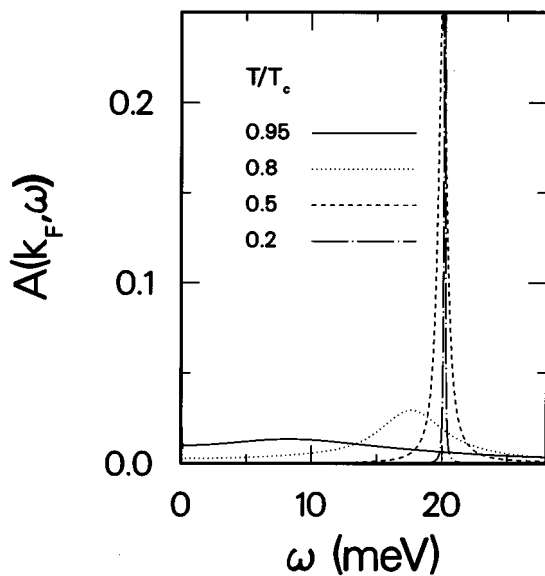


Fig. 7. Single-particle spectral function $A(k_F, \omega)$ at the Fermi surface versus frequency in the clean limit, for various reduced temperatures. The spectral function is considerably broadened near T_c , due to temperature alone. At the two lowest temperatures shown, while there is no true gap in the excitation spectrum, this plot makes it clear that, practically speaking, an effective gap in the excitation spectrum is present. A Debye electron-phonon spectrum was used with $\lambda = 1$ and cutoff frequency $\omega_D = 30$ meV.

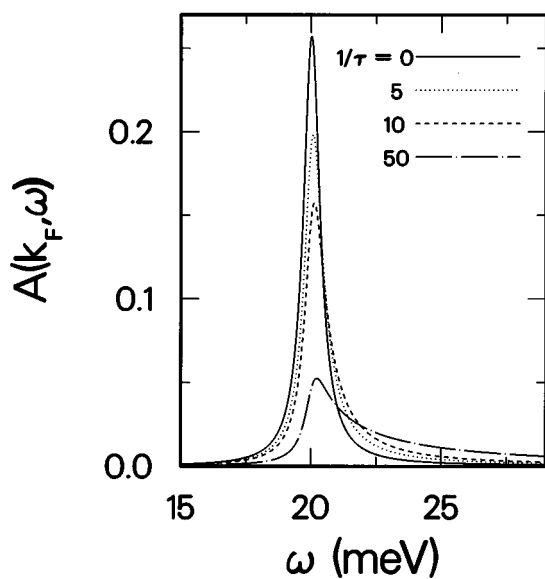


Fig. 8. Single-particle spectral function $A(k_F, \omega)$ at the Fermi surface versus frequency for various impurity scattering rates, as indicated. Note the broadening which occurs with increasing impurity scattering. However, spectral weight remains absent in the 'gap region'. Results are for a temperature $T/T_c = 0.5$, and with a Debye electron-phonon spectrum with $\lambda = 1$ and cutoff frequency $\omega_D = 30$ meV.

it remains a useful indicator of the scattering rate for energies up to about the gap energy.

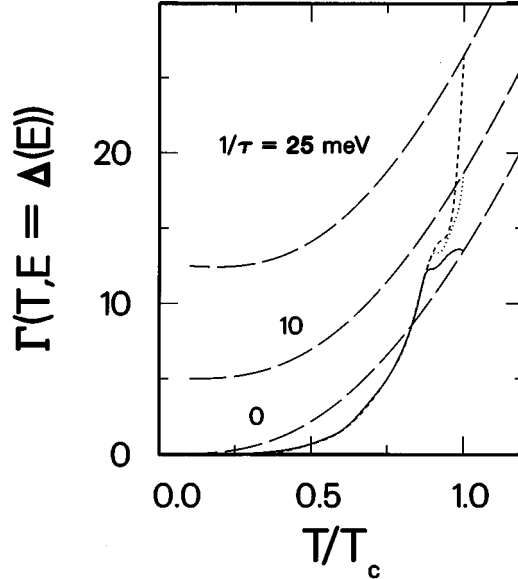


Fig. 9. Quasiparticle scattering rate $\Gamma(T, E=\Delta(E))$, evaluated at the quasiparticle energy, given on the Fermi surface by $E = \Delta(E)$, versus T/T_c for various impurity scattering rates $1/\tau$ in both the superconducting and normal (long-dashed curves) states. These results are in quantitative agreement with those in Fig. 6, since the energy scale Δ is still small compared to other (phonon) energy scales in the problem. In particular, below about $0.8T_c$, the scattering rate is independent of the amount of impurity scattering present in the normal state. A Debye electron-phonon spectrum was used with $\lambda = 1$ and cutoff frequency $\omega_D = 30$ meV.

3. Optical Conductivity

(3a) Extraction of a Scattering Rate from the Conductivity

Using the Kubo formalism (Mahan 1981, 1987), the optical conductivity can be related to a current-current correlation function. The final result for the frequency dependence of the conductivity in the long wavelength limit is (Nam 1967; Lee *et al.* 1989; Bickers *et al.* 1990; Marsiglio *et al.* 1992)

$$\sigma(\nu) = \frac{i}{\nu} \left(\Pi(\nu + i\delta) + \frac{n e^2}{m} \right), \quad (26)$$

where the paramagnetic response function $\Pi(\nu + i\delta)$ is given in the previous article (Marsiglio and Carbotte 1997, see p. 975), and will not be repeated here.

To summarise the theoretical framework within which we are working: for a given model for the spectral density, $\alpha^2 F(\nu)$ and a choice of impurity scattering rate $1/\tau$, we can compute the conductivity $\sigma(\nu)$ at any frequency and temperature, including effects due to both elastic and inelastic scattering mechanisms, the latter being determined by the choice of electron-phonon spectral density. As explained in the introduction, however, vertex corrections are omitted.

In the analysis of experimental data it is possible to use several methods to extract a single temperature dependent scattering rate. One such method utilised the microwave conductivity in $\text{YBaCu}_3\text{O}_{7-x}$ (Bonn *et al.* 1992, 1993) and in Nb (Klein 1994), and adopted a two-fluid model description of the superconducting state. It was assumed that the absorptive component of the conductivity [real part of σ at finite frequency, denoted by $\sigma_1(\nu)$] was due only to the normal component of the fluid. Thus an expression of the form

$$\sigma_1(\nu, T) = \frac{ne^2}{m} \frac{m}{m^*(T)} \left[1 - \frac{\lambda^2(0)}{\lambda^2(T)} \right] \frac{\tau(T)}{1 + (\nu\tau(T))^2} \quad (27)$$

is assumed to hold approximately. In equation (27) $\tau(T)$ has units of a scattering time and $\lambda(T)$ is the penetration depth at temperature T . Here we will calculate $\sigma_1(\nu, T)$ for a model $\alpha^2 F(\nu)$ and $1/\tau$ using the full expression (26). At the same time we can calculate the penetration depth, either from a zero frequency limit of (26), or directly from the imaginary axis (Nam 1967; Carbotte 1990; Marsiglio *et al.* 1990):

$$\frac{\lambda^2(0)}{\lambda^2(T)} = \pi T \sum_{m=-\infty}^{\infty} \frac{\phi_m^2}{(\omega_m^2 Z^2(i\omega_m) + \phi_m^2)^{\frac{3}{2}}}. \quad (28)$$

The idea is to examine the zero frequency limit of (27), and thus define a scattering rate relative to the rate at T_c (Klein 1994):

$$\frac{\tau(T_c)}{t(T)} \equiv \left(1 - \frac{\lambda^2(0)}{\lambda^2(T)} \right) \frac{\sigma_N(T_c)}{\sigma_1(T)}, \quad (29)$$

where it has been assumed that the mass enhancement factor in (27) does not change with temperature. In this way an effective scattering rate was extracted from microwave data for $\text{YBaCu}_3\text{O}_{7-x}$ (Bonn *et al.* 1992, 1993) and Nb (Klein 1994).

To see how closely this scattering rate follows the quasiparticle scattering rate, we show results in Fig. 10 for $\tau(T_c)/\tau(T)$ defined by (29) in the superconducting state (solid curve) with which we compare the inverse quasiparticle lifetime for both the normal (short-dashed curve, equation 9), and the superconducting (long-dashed curve, equation 6) states. The results are based on a Debye model spectrum for $\alpha^2 F(\nu)$ used in the previous section, with mass enhancement parameter $\lambda = 1$ and $T_c = 100$ K. (A negative μ^* is required.) Note that the normal state scattering rate (short-dashed curve) is only sensitive to the low frequency part of $\alpha^2 F(\nu)$ at low temperatures: a ν^2 dependence in $\alpha^2 F(\nu)$ implies a T^3 dependence in $1/\tau(T)$. [Again, vertex corrections would alter this to the familiar T^5 law (Ashcroft and Mermin 1976).] The agreement between the inverse lifetime (long-dashed curve) and the scattering rate defined by the two-fluid model (solid curve) in the superconducting state is remarkable, although later we shall see that this quantitative agreement occurs only with this particular Debye spectrum. This indicates that the two-fluid description makes sense (Berlinsky *et al.* 1993; Bonn *et al.* 1994) at least qualitatively, and the quantities shown

in Fig. 10 apply to the normal component of the superfluid. Fig. 10 illustrates the comparison in the clean limit, where the two-fluid description is expected to be most accurate (Bonn *et al.* 1994). Before investigating impurity dependence, we turn to a second possible procedure for extracting a scattering rate from conductivity data (Romero *et al.* 1992; Tanner and Timusk 1992), which is simply a generalisation of that used by Shulga *et al.* (1991) and Dolgov *et al.* (1991) to the superconducting state. One simply fits the low frequency absorptive part of the conductivity to a Drude form:

$$\sigma_1(\nu, T) = \frac{ne^2}{m} \frac{1}{m^*/m} \frac{\tau^*(T)}{1 + (\nu\tau^*)^2}. \quad (30)$$

As described in Shulga *et al.* (1991), Dolgov *et al.* (1991) and Marsiglio and Carbotte (1995), it is possible to fit a Drude form to the low frequency part of the optical conductivity in the normal state. Such a fit is also possible in the superconducting state (Romero *et al.* 1992). Theoretically, the fit is problematic in a BCS approach because there is a Hebel–Slichter logarithmic singularity at low frequency *at all temperatures in the superconducting state*. However, with the Eliashberg approach, the Hebel–Slichter singularity is smeared, and one can fit a Drude form over a limited range of frequency. Such a fit for a Debye spectrum is also included in Fig. 10 (dotted curve). While the fit is in qualitative agreement with the inverse lifetime, this method of characterising the inverse lifetime in

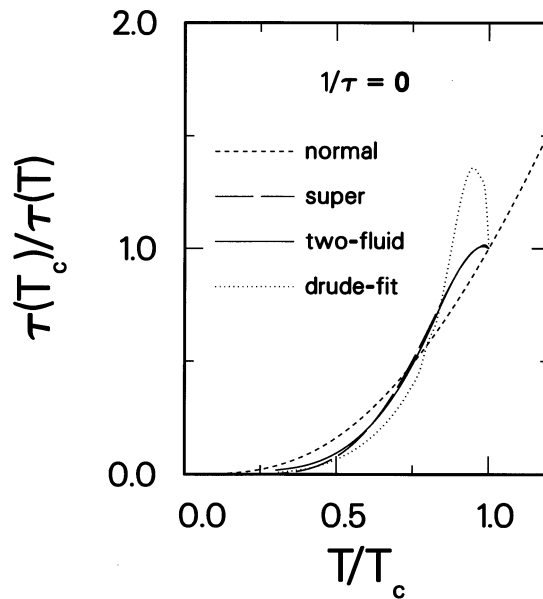


Fig. 10. Various normalised scattering rates versus reduced temperature. The normal and superconducting scattering rates come from the quasiparticle inverse lifetime, given by equation (6), at zero energy. The two-fluid result comes from (29) while the Drude fit is obtained by fitting (30) to the low frequency conductivity in the superconducting state. Note the agreement of the scattering rate as extracted from the two-fluid analysis with the inverse lifetime in the superconducting state. A Debye electron–phonon spectrum was used with $\lambda = 1$ and cutoff frequency $\omega_D = 30$ meV.

the superconducting state is clearly not as accurate as the two-fluid model. The fits themselves are shown in Fig. 11. It is clear that the fits fail at sufficiently high frequency, as one would expect, but that they characterise well the low frequency response in the superconducting state.

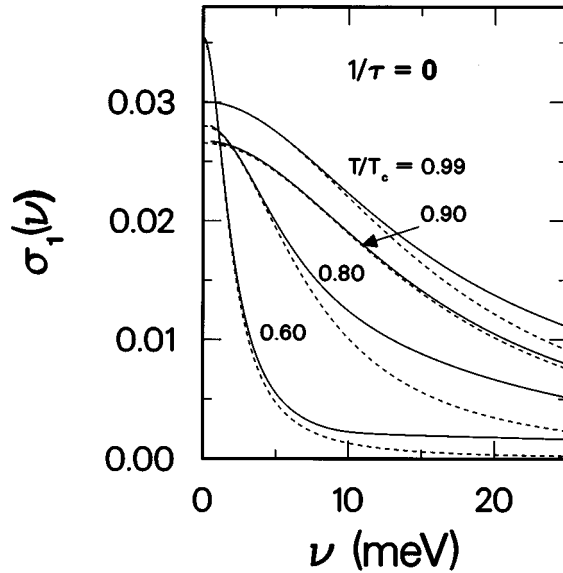


Fig. 11. Low frequency conductivity in the superconducting state (solid curves) along with their fits based on equation (30) (dashed curves). These fits were used in Fig. 10 (dotted curves).

Fig. 10 clearly shows that there is considerable freedom and hence ambiguity in extracting a temperature dependent scattering rate from conductivity data. Nevertheless, in the clean limit it is evident that the two-fluid model is a useful device for extracting the low energy inverse quasiparticle lifetime in the superconducting state.

With the addition of impurities the situation changes considerably. This is illustrated in Fig. 12, where the same calculations as in Fig. 10 are shown, but with an additional impurity scattering, $1/\tau = 25$ meV, included. The use of formula (27), inspired by the two-fluid model, gives a scattering rate (solid curve) that falls much less rapidly around $T = T_c$ than does the inverse quasiparticle lifetime in the superconducting state (long-dashed curve). The latter curve drops almost vertically as the temperature drops below T_c , as has already been discussed. The result based on the Drude fit (dotted curve) shows a peak which is reduced in size from that in the clean limit (Fig. 10). Indeed, for increased impurity scattering, the peak just below T_c disappears. In both cases a rapid suppression is expected just below T_c : in the case of the inverse lifetime, this suppression is a consequence of Anderson's (1959) theorem, as already discussed. In the case of the Drude fit, it is easy to see that this is the case in the dirty limit. In the dirty limit the conductivity is almost flat as a function of frequency on the scale of $1/\tau$, at T_c . Just below T_c , however, a gap in the spectrum begins to develop, so that weight is shifted from roughly the gap region to the delta function at

the origin. Any low energy fit will then use a Lorentzian width which senses this depression in the conductivity, which is on an energy scale of the gap. This represents a significant suppression from the normal state scattering rate (infinite in the dirty limit). Here we are in an intermediate regime, with $1/\tau = 25$ meV [note: $\Delta(T=0) = 20.2$ meV]. The corresponding fits for Fig. 12 are shown in Fig. 13.

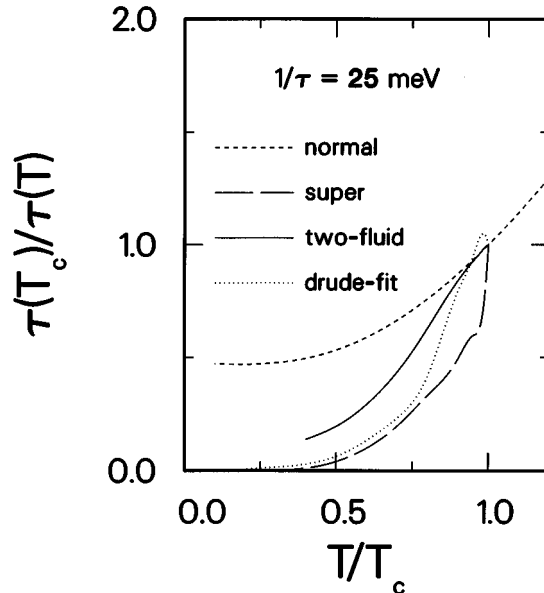


Fig. 12. Same as Fig. 10, except now with an impurity scattering rate of 25 meV. Note that the two-fluid analysis agrees poorly with the quasiparticle inverse lifetime.

(3b) Possible Origin of the Low Temperature Conductivity Peak

As an aside we wish to further examine the low frequency conductivity versus reduced temperature, a quantity measured in the high T_c oxides by microwave techniques (Nuss *et al.* 1991; Bonn *et al.* 1992, 1994). In these experiments a peak was observed in the real part of the low frequency conductivity as a function of temperature, the origin of which has been discussed in many contexts. Here, we add yet another possibility. In Fig. 14 we show the real part of the conductivity $\sigma_1(\nu)$ versus reduced temperature, for several low frequencies. We continue to use a model Debye spectrum to simply establish qualitative effects. Note the relative insensitivity to frequency, a feature of strong coupling pointed out in Marsiglio (1991). Also note the lack of a coherence peak just below T_c . Nonetheless, a broad peak exists at lower temperatures, somewhat reminiscent of that observed in $\text{YBaCu}_3\text{O}_{7-x}$ (Nuss *et al.* 1991; Bonn *et al.* 1992, 1994). This peak exists because of a competition between an increasing scattering time (making σ increase) and a decreasing normal component (making σ decrease, particularly as $T \rightarrow 0$). We should note that this peak is most prominent in the clean limit. As Fig. 13 indicates (see values at the intercept), the peak is absent for a sufficiently large impurity scattering rate.

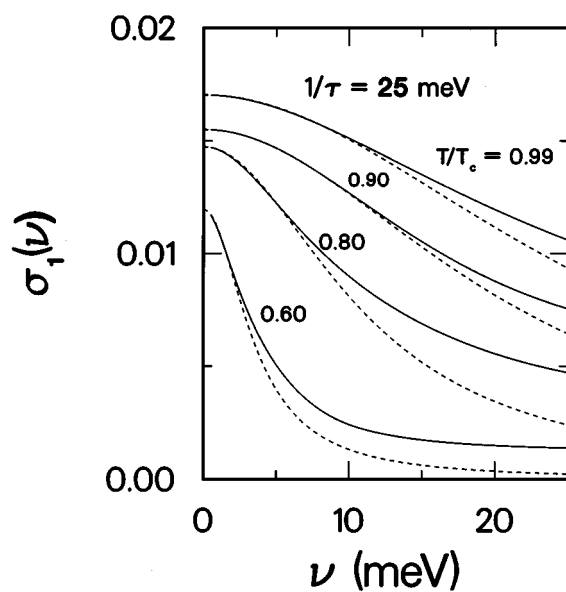


Fig. 13. Low frequency conductivity fits used in Fig. 12.

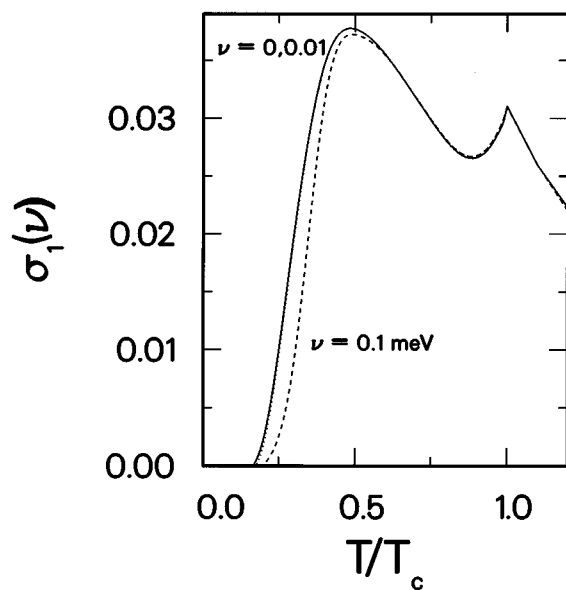


Fig. 14. Very low frequency conductivity as a function of reduced temperature, in the clean limit. A Debye electron-phonon spectrum was used with $\lambda = 1$ and cutoff frequency $\omega_D = 30$ meV. Note that the results are relatively insensitive to frequency (the $\nu = 0.01$ meV result, given by the dotted curve, is essentially hidden by the zero frequency result). A microwave experiment yields essentially zero frequency results.

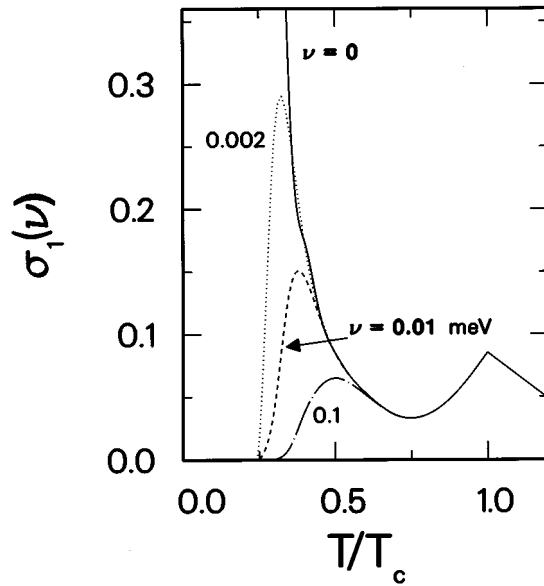


Fig. 15. Same as for Fig. 14, but now with the triangular spectrum as described in the text. Note that the zero frequency conductivity appears to diverge as $T \rightarrow 0$. A microwave experiment will yield a large low temperature peak as a function of reduced temperature, whose magnitude will depend strongly on the frequency. These results are for the clean limit. The peak is also reduced as impurity scattering is added (not shown).

It is of interest to examine what dependence these results have on the electron–phonon spectral function. As an extreme we utilise a spectrum which is sharply peaked at some high frequency and, in contrast to the Debye model employed above, coupling to low frequency modes is absent; such a spectrum models a strong coupling to an optic mode. We choose a triangular shape for convenience, starting at $\omega_0 = 34.8$ meV with a cutoff at $\omega_E = 35.5$ meV. The coupling constant is chosen so that the mass enhancement value is $\lambda = 1$, in agreement with that chosen for the Debye spectrum. As was the case there, a negative μ^* is used to give $T_c = 100$ K, and the zero temperature gap was found to be close to the Debye value.

In Fig. 15 we plot the real part of the low frequency conductivity $\sigma_1(\nu)$ versus reduced temperature, now using the triangular spectrum for $\alpha^2 F(\nu)$. In contrast to the result for the Debye model, the low frequency conductivity is strongly frequency dependent at low temperatures. In fact, for $\nu = 0$, the conductivity appears to diverge. We believe that at sufficiently low temperature, this curve will actually achieve a maximum and approach zero at zero temperature, but we have been unable to obtain this result numerically. Once again there is a competition between an increasing scattering time and a decreasing normal density component as the temperature is lowered from T_c . Here, however, the increasing scattering time appears to be overwhelming the decrease in normal fluid density. The key difference with the Debye spectrum is that here the spectrum has a big gap, so that the lifetime is increasing exponentially with decreasing temperature, already in the normal state. Recall that in the Debye case the increase followed a power law behaviour with decreasing temperature. Since the decrease in normal fluid

density is always exponential, this term dominates in the Debye case, whereas in the case of the gapped spectrum the competition is subtle, and will depend strongly on the details of the spectrum (an electron-phonon spectrum with a much smaller gap will yield a zero frequency conductivity which approaches zero at zero temperature, for example).

The physics of this conductivity peak is different from what has been already proposed for $\text{YBaCu}_3\text{O}_{7-x}$. It has been suggested that the excitation spectrum *becomes gapped due to the superconductivity*, i.e. a feedback mechanism exists which creates a low frequency gap in the excitation spectrum as the superconducting order parameter opens up below T_c . Such a scenario has been explored within a marginal Fermi liquid scheme (Nuss *et al.* 1991; Nicol and Carbotte 1991*a*, 1991*b*), and is also consistent with thermal conductivity experiments (Yu *et al.* 1992). Here the conductivity peak arises because the spectrum is already gapped, and the scattering rate is sufficiently high at T_c because T_c itself is fairly high. We should warn the reader that this mechanism requires a ‘fine tuning’ of the spectrum, i.e. a large gap is required in the phonon spectrum. An alternate boson spectrum may be operative, and then a less extreme boson spectrum may work, if the normal state electron density falls at a correspondingly slower rate as the temperature is lowered. This would be achieved if the superconducting order parameter has nodes, for example (Schachinger *et al.* 1996).

Note that for any non-zero frequency the conductivity has a visible maximum, and quickly approaches zero at sufficiently low temperature. Nonetheless this turn around occurs for yet another reason: as one lowers the temperature the

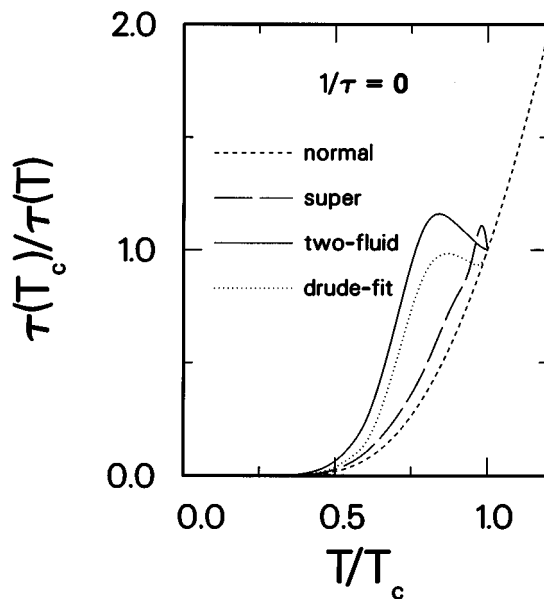


Fig. 16. Comparison of scattering rates (as in Fig. 10) calculated for the triangular spectrum, in the clean limit. Note that the normal state result approaches $T = 0$ exponentially due to the gap in the $\alpha^2 F(\nu)$ spectrum (in Fig. 10 the corresponding curve approached zero with a power law behaviour). While the results in the superconducting state are qualitatively similar, they no longer agree quantitatively with one another, as in Fig. 10.

Drude-like peak at low frequencies gets narrower while at the same time the magnitude of the zero temperature intercept increases. For any given finite frequency then, a temperature is eventually reached below which this frequency is now on the tail of the Drude-like peak. This means that while the zero frequency conductivity increases, that at any finite frequency will eventually decrease as the width becomes smaller than the frequency. So in this case the increase in scattering lifetime still dominates the decrease in normal fluid density, but, because we are fixed at a finite frequency, the conductivity decreases. Note that frequencies of order 0.01 meV ($\approx 2.4 \text{ GHz}$) are within the range of microwave frequencies that are used in experiments.

To show this more explicitly we illustrate in Fig. 16 the various scattering rates obtained with the gapped spectrum. These are to be compared with those shown for the Debye model in Fig. 10. Clearly the quantitative agreement between the scattering rate inspired by the two-fluid model and the inverse lifetime that was seen in Fig. 10 with the Debye spectrum was fortuitous. While a qualitative correspondence between these two entities continues to exist with the gapped spectrum, they are no longer in quantitative agreement. We have verified that this is generically true, by investigating other spectra, not shown here.

4. Summary

We have investigated the quasiparticle lifetime in an Eliashberg s-wave superconductor, generalising earlier work (Kaplan *et al.* 1976) to include impurity scattering as well. We find that the quasiparticle lifetime becomes infinite at low temperatures, independent of the impurity scattering rate, which we understand as simply a manifestation of Anderson's (1959) theorem. Thus, on general grounds, within a BCS framework, the inverse quasiparticle lifetime should collapse to zero in the superconducting state. We have also emphasised the importance of the so-called coherence factors for the single-particle spectral function, when impurity scattering is included within the BCS case.

Two methods have been investigated for extracting the scattering rate from the low frequency conductivity. One relies on a two-fluid model picture, and the other simply utilises a low frequency Drude fit. Neither should necessarily correspond very closely to the quasiparticle inverse lifetime, and we find that in general they do not, quantitatively. Qualitatively, however, the scattering rate defined by either procedure gives the correct temperature dependence for the inverse lifetime. In the presence of impurities, the two-fluid prescription appears to be less accurate, presumably because such a prescription takes into account only the lower normal fluid density as the temperature is lowered, and not the fact that impurity scattering is less effective in the superconducting state. Thus we caution that the interpretation of a conductivity-derived scattering rate as a quasiparticle inverse lifetime, while qualitatively correct, is quantitatively inaccurate.

References

- Allen, P. B., and Mitrović, B. (1982). In 'Solid State Physics', Vol. 37 (Eds H. Ehrenreich *et al.*), p. 1 (Academic: New York).
- Allen, P. B., and Rainer, D. (1991). *Nature* **349**, 396.
- Anderson, P. W. (1959). *J. Phys. Chem. Solids* **11**, 26.

- Ashcroft, N. W., and Mermin, N. D. (1976). 'Solid State Physics' (Holt, Rinehart and Winston: Philadelphia).
- Bedell, K. S., Coffey, D., Meltzer, D. E., Pines, D., and Schrieffer, J. R. (1990). In 'High Temperature Superconductivity: The Los Alamos Symposium' (Addison-Wesley: Don Mills).
- Berlinsky, A. J., Kallin, C., Rose, G., and Shi, A.-C. (1993). *Phys. Rev. B* **48**, 4074.
- Bickers, N. E., Scalapino, D. J., Collins, T., and Schlessinger, Z. (1990). *Phys. Rev. B* **42**, 67.
- Bonn, D. A., Dosanjh, P., Liang, R., and Hardy, W. N. (1992). *Phys. Rev. Lett.* **68**, 2390.
- Bonn, D. A., Liang, R., Riseman, T. M., Baar, D. J., Morgan, D. C., Zhang, K., Dosanjh, P., Duty, T. L., MacFarlane, A., Morris, G. D., Brewer, J. H., Hardy, W. N., Kallin, C., and Berlinsky, A. J. (1993). *Phys. Rev. B* **47**, 11314.
- Bonn, D. A., Zhang, K., Kamal, S., Liang, R., Dosanjh, P., Hardy, W. N., Kallin, C., and Berlinsky, A. J. (1994). *Phys. Rev. Lett.* **72**, 1391.
- Carbotte, J. P. (1990). *Rev. Mod. Phys.* **62**, 1027.
- Dolgov, O. V., Maksimov, E. G., and Shulga, S. V. (1991). In 'Electron-Phonon Interaction in Oxide Superconductors' (Ed. R. Baquero), p. 30 (World Scientific: Singapore).
- Eliashberg, G. M. (1960). *Zh. Eksperim. i Teor. Fiz.* **38**, 966; *Sov. Phys. JETP* **11**, 696.
- Grimvall, G. (1981). 'The Electron-Phonon Interaction in Metals' (North Holland: New York).
- Hebel, L. C., and Slichter, C. P. (1959). *Phys. Rev.* **113**, 1504.
- Kaplan, S. B., Chi, C. C., Langenberg, D. N., Chang, J. J., Jafarey, S., and Scalapino, D. J. (1976). *Phys. Rev. B* **14**, 4854.
- Karakozov, A. E., Maksimov, E. G., and Mashkov, S. A. (1975). *Zh. Eksp. Teor. Fiz.* **68**, 1937; *Sov. Phys. JETP* **41**, 971 (1976).
- Klein, O. (1994). *Phys. Rev. Lett.* **72**, 1390.
- Lee, W., Rainer, D., and Zimmermann, W. (1989). *Physica C* **159**, 535.
- Mahan, G. D. (1981). 'Many-Particle Physics' (Plenum: New York).
- Mahan, G. D. (1987). *Phys. Reports* **145**, 251.
- Marsiglio, F. (1991). *Phys. Rev. B* **44**, 5373.
- Marsiglio, F., and Carbotte, J. P. (1991). *Phys. Rev. B* **43**, 5355.
- Marsiglio, F., and Carbotte, J. P. (1995). *Phys. Rev. B* **52**, 16192.
- Marsiglio, F., and Carbotte, J. P. (1997). *Aust. J. Phys.* **50**, 975.
- Marsiglio, F., Akis, R., and Carbotte, J. P. (1992). *Phys. Rev. B* **45**, 9865.
- Marsiglio, F., Carbotte, J. P., and Blezius, J. (1990). *Phys. Rev. B* **41**, 6457.
- Marsiglio, F., Carbotte, J. P., Puchkov, A., and Timusk, T. (1996). *Phys. Rev. B* **53**, 9433.
- Marsiglio, F., Schossmann, M., and Carbotte, J. P. (1988). *Phys. Rev. B* **37**, 4965.
- Nam, S. B. (1967). *Phys. Rev. B* **156**, 470; 487.
- Narayanamurti, V., Dynes, R. C., Hu, P., Smith, H., and Brinkman, W. F. (1978). *Phys. Rev. B* **18**, 6041.
- Nicol, E. J. (1991). PhD thesis, McMaster University, unpublished.
- Nicol, E. J., and Carbotte, J. P. (1991a). *Phys. Rev. B* **44**, 7741.
- Nicol, E. J., and Carbotte, J. P. (1991b). *Physica C* **185**, 162.
- Nuss, M. C., Mankiewich, P. M., O'Malley, M. L., Westerwick, E. H., and Littlewood, P. B. (1991). *Phys. Rev. Lett.* **66**, 3305.
- Owen, C. S., and Scalapino, D. J. (1971). *Physica* **55**, 691.
- Pethick, C. J., and Pines, D. (1986). *Phys. Rev. Lett.* **57**, 118.
- Rainer, D., and Bergmann, G. (1974). *J. Low Temp. Phys.* **14**, 501.
- Romero, D. B., Porter, C. D., Tanner, D. B., Forro, L., Mandrus, D., Mihaly, L., Carr, G. L., and Williams, G. P. (1992). *Phys. Rev. Lett.* **68**, 1590.
- Scalapino, D. J. (1969). In 'Superconductivity', Vol. 1 (Ed. R. D. Parks), p. 449 (Marcel Dekker: New York).
- Schachinger, E., Carbotte, J. P., and Marsiglio, F. (1977). *Phys. Rev. B* **56**, 2738.
- Schrieffer, J. R. (1983). 'Theory of Superconductivity', p. 122 (Benjamin/Cummings: Don Mills).
- Shulga, S. V., Dolgov, O. V., and Maksimov, E. G. (1991). *Physica C* **178**, 266.
- Tanner, D. B., and Timusk, T. (1992). In 'Physical Properties of High Temperature Superconductors III' (Ed. D. M. Ginsberg), p. 363 (World Scientific: Singapore).
- Yu, R. C., Salamon, M. B., Lu, J. P., and Yee, W. C. (1992). *Phys. Rev. Lett.* **69**, 1431.